A Tractable Statistical Representation of IFTR Fading With Applications

Maryam Olyaee, Hadi Hashemi, and Juan M. Romero-Jerez, *Senior Member, IEEE*

***Abstract*— The recently introduced independent fluctuating two-ray (IFTR) fading model, consisting of two specular components fluctuating independently plus a diffuse component, has proven to provide an excellent fit to different wireless environments, including the millimeter-wave band. However, the original formulations of the probability density function (PDF) and cumulative distribution function (CDF) of this model are not applicable to all possible values of its defining parameters, and are given in terms of multifold generalized hypergeometric functions, which prevents their widespread use for the derivation of performance metric expressions. A new formulation of the IFTR model is here presented as a countable mixture of Gamma distributions which greatly facilitates the performance evaluation for this model in terms of the metrics already known for the much simpler and widely used Nakagami-m fading, and is shown to provide a better fit to empirical measurements than the original formulation. Additionally, a closed-form expression is presented for the generalized moment generating function (GMGF), which permits to readily obtain all the moments of the distribution of the model, as well as several relevant performance metrics. Based on these new derivations, performance results are presented for the IFTR model considering different metrics, which are verified by Monte Carlo simulations.**

***Index Terms*— Multipath fading, independent fluctuating two-ray (IFTR), Gamma distribution, generalized moment generating function.**

I. Introduction

THE new challenges and use cases envisioned in the 6G framework require the adoption of new and extended capabilities in wireless communications networks [1]. Thus, new services and applications requiring extremely high-data-rate, hyper reliability and low latency, high-resolution imaging, and high-precision positioning demand for peak data rates and spectrum efficiency higher than in 5G services such as enhanced Mobile Broadband (eMBB), Ultra-Reliable Low-Latency Communications (URLLC) and massive Machine-Type Communications (mMTC) [2]. Additional usage scenarios such as immersive communication and integration of sensing/AI and communication are also envisioned in 6G networks. These new scenarios and requirements demand for higher bandwidths, which are available at the mmWave and even sub-THz/THz bands, in which the fundamental propagation characteristics need to be understood and for which it is of paramount importance to develop accurate channel models for network planning and preliminary evaluation. In this regard, channel multipath fading is an essential propagation effect to be considered due to the potential detrimental impact on performance. Therefore, accurate characterization of wireless channel fading at those higher frequencies has become a relevant research topic, and much effort is being made in this area [3], [4], [5]. Theoretical statistical channel models are fundamental tools for evaluating the performance of wireless networks and can also help to reduce the high computational load of software network simulations [6].

Recently, the independent fluctuating two-ray (IFTR) [7] channel model has been presented to characterize multipath propagation, which includes several well-known distributions, namely Rayleigh, Rician, Hoyt (Nakagami-q), Rician Shadowed, and Nakagami-m, as special or limiting cases. The IFTR model consists of two dominant (specular) waves plus a diffuse component, due to the aggregation of multiple low-power scattered waves, modeled as a complex Gaussian random variable (RV), where the specular components are assumed to fluctuate independently following Nakagami-m fading. This model is related to the fluctuating two-ray (FTR) fading model except that in the latter the two specular components are assumed to be fully correlated and fluctuate simultaneously. The FTR model was introduced in [8] and was later reformulated in [9] and [10] and, more recently, in [11], and has been studied abundantly for different wireless environments, mostly in the context of millimeter-wave communications, and considering many different performance metrics (see for example [11] and the references therein). In spite of the apparent similitude in the formal definition of the FTR and IFTR fading models, there are major differences between them, both in terms of the fitting results to experimental measurements and in the involved mathematical derivations. On the one hand, the IFTR fading model has been shown to provide a (sometimes

Manuscript received 5 December 2023; revised 16 February 2024; accepted 10 March 2024. Date of publication 18 March 2024; date of current version 16 August 2024. This work has been funded in part by Junta de Andalucia through project P21-00420 and also grant EMERGIA20-00297, and in part by MCIN/AEI/10.13039/501100011033 through grant PID2020-118139RB-I00. Funding for open access charge: Universidad de Málaga / CBUA. Part of this work has been submitted for consideration to be presented at the 2024 IEEE International Symposium on Information Theory. The associate editor coordinating the review of this article and approving it for publication was J. Zhang. *(Corresponding author: Juan M. Romero-Jerez.)*

Maryam Olyaee and Juan M. Romero-Jerez are with the Communications and Signal Processing Laboratory, Telecommunication Research Institute (TELMA), ETSI Telecomunicación, Universidad de Málaga, 29010 Málaga, Spain (e-mail: olyaee@uma.es; romero@dte.uma.es).

Hadi Hashemi is with the Department of Signal Theory, Networking and Communications, Universidad de Granada, 18071 Granada, Spain (e-mail: hashemi@ugr.es).

Color versions of one or more figures in this article are available at https://doi.org/10.1109/TCOMM.2024.3377702.

Digital Object Identifier 10.1109/TCOMM.2024.3377702

remarkable) better fit than FTR fading (as well as other generalized fading models such as κ-μ shadowed [12] and two-wave with diffuse power –TWDP– [11]) to experimental data in very different environments, including line-of-sight (LOS) millimeter-wave, land-mobile satellites (LMS), and underwater acoustic communications (UAC) [7]. On the other hand, the independence of the two specular components in the IFTR model imposes new mathematical challenges, as now a two-fold nested integration always appear in its statistical characterization, which cannot be obtained from that for the FTR model, as different trascendental functions are involved, and requires a separate analysis. It must be noted that both models are complementary and typically applicable to different situations that can be found in real environments, i.e, fully correlated (FTR) versus independent (IFTR) fluctuations of the specular components.

Although both the probability density function (PDF) and cumulative distribution function (CDF) of the IFTR model were presented in [7], their use is rather limited for two reasons: on the one hand they are not completely general, as they require assuming one of the model parameters m_1 or m_2 to be integer, while they can take any arbitrary positive real value in realistic propagation scenarios; on the other hand, the known PDF and CDF are given in terms of a generalized hypergeometric function, which is actually a multifold infinite summation, which is very difficult to manipulate to obtain analytical expressions for most performance metrics in wireless communication systems.

In this paper, we solve the aforementioned issues by deriving a new statistical characterization of the IFTR fading model assuming arbitrary positive values of m_1, m_2 and easy to manipulate. Additionally, we expand the known results for the precise characterization of the model and apply them for the performance analysis of wireless systems. Specifically, the key contributions of this paper are:

- A new formulation is presented for the PDF and CDF of the instantaneous SNR of IFTR fading in terms of an infinite countable mixture of Gamma distributions for arbitrary values of the channel parameters m_1 and m_2, where the weights of the elements of the mixture are given in closed-form. The resulting statistical functions are much easier to manipulate mathematically than previous known expressions, and many performance metrics of fading channels which can be expressed as a weighted sum of Gamma distributions are known [13]. Also, the new formulation is shown to provide a better fit to empirical measurements than the original one.
- It is demonstrated that any average performance metric expression already known for Nakagami-m fading (for which there is a vast literature) allows to obtain such metric for IFTR fading in a straightforward manner. Also, the obtained infinite series are demonstrated to be convergent and are precisely truncated and evaluated using the Kolmogorov-Smirnov (KS) goodness-of-fit test.
- The generalized moment generating function (GMGF) of the IFTR fading model is obtained for the first time, which for many relevant cases can be written in closed-form, allowing to obtain all the moments of the distribution. In spite of the model generality and statistical complexity, this function permits to obtain closed-form expressions for different relevant performance metrics including, for example, outage probability under interference and energy detection probability.
- The new and expanded statistical characterization of IFTR fading is used for its performance analysis evaluation in terms of the average capacity, ergodic mutual information for discrete inputs, outage probability with and without interference, secrecy capacity outage probability and average bit error rate (BER) for different modulations. The effect of the parameters values of the model are evaluated numerically and verified by simulation.

The rest of this paper is organized as follows: The channel model is presented in Section II. Then, in Section III, the new representation of the IFTR fading is presented, as well as, for the first time, to the authors' knowledge, an expression of the GMGF, which for many relevant cases can be written in closed-form. Several performance metrics, including the average channel capacity, the ergodic mutual information for discrete inputs, the outage probability, the secrecy capacity outage probability and the BER in IFTR fading are analyzed in Section IV. Simulation and numerical results are given in Section V. Finally, the paper is concluded in Section VI.

II. Preliminary Definitions and Channel Model

Definition 1: A RV X following a Gamma distribution with shape parameter λ and scale parameter ν will be denoted as $X \sim \mathcal{G}(\lambda, \nu)$, and its PDF and CDF are given, respectively, by

$$f^{\mathcal{G}}(x;\lambda,\nu) = \frac{x^{\lambda-1}}{\Gamma(\lambda)\nu^{\lambda}} e^{-\frac{x}{\nu}}, \tag{1}$$

$$F^{\mathcal{G}}(x;\lambda,\nu) = \frac{1}{\Gamma(\lambda)} \gamma\left(\lambda, \frac{x}{\nu}\right), \tag{2}$$

where $\gamma(\cdot,\cdot)$ is the incomplete Gamma function [14, eq. (8.350.1)].

Remark 1: The SNR $\gamma_{\mathcal{K}}$ (or, equivalently, the received power) in a Nakagami-m fading with mean $\bar{\gamma}_{\mathcal{K}}$ and fading severity parameter m follows a Gamma distribution with shape parameter m and scale parameter $\bar{\gamma}_{\mathcal{K}}/m$, i.e., $\gamma_{\mathcal{K}} \sim \mathcal{G}(m, \bar{\gamma}_{\mathcal{K}}/m)$.

The IFTR fading model is composed of two specular waves, whose amplitude fluctuate according to independent Nakagami-m fading, plus an undetermined number of scattered low-amplitude waves (the diffuse component) which, by virtue of the central limit theorem, are jointly represented by a complex Gaussian RV. Let $\zeta_i \sim \mathcal{G}(m_i, 1/m_i)$, with $i \in \{1,2\}$, then the complex base-band representation of the IFTR fading model can be expressed as

$$V_r = \sqrt{\zeta_1} V_1 e^{j\phi_1} + \sqrt{\zeta_2} V_2 e^{j\phi_2} + X + jY, \tag{3}$$

where V_i is the average amplitude of the i-th specular component, ϕ_i is a uniformly distributed RV in $[0, 2\pi)$ representing its phase, and $X + jY$ models the diffuse component with $X, Y \sim \mathcal{N}(0, \sigma^2)$.

In addition to the fading severity parameters of the specular components, m_1 and m_2, the IFTR model will be determined by the following physically-motivated parameters:

$$K = \frac{V_1^2 + V_2^2}{2\sigma^2}, \tag{4}$$

$$\Delta = \frac{2V_1V_2}{V_1^2 + V_2^2}, \tag{5}$$

where K represents the ratio of the average power of the dominant components to the power of the diffuse component and $\Delta \in [0,1]$ provides a measure of the specular components similarity, so that $\Delta = 1$ implies $V_1 = V_2$. Without loss of generality we will assume $V_1 \geq V_2$, and therefore $\Delta = 0$ implies $V_2 = 0$, i.e., only the first specular component, if any, is received. For the sake of compactness in subsequent expressions, we will also define the following ancillary parameters, given in terms of K and Δ:

$$K_1 \triangleq \frac{V_1^2}{2\sigma^2} = K\frac{1+\sqrt{1-\Delta^2}}{2}, \tag{6}$$

$$K_2 \triangleq \frac{V_2^2}{2\sigma^2} = K\frac{1-\sqrt{1-\Delta^2}}{2}. \tag{7}$$

The IFTR model is very versatile and includes different classical and generalized fading models as particular cases by an appropriate selection of the parameters. Thus, for $m_1, m_2 \to \infty$ the fluctuations of the specular components disappear and the IFTR model tends to the TWDP one [15]. If, in addition, we let $\Delta = 0$, the Rice model is obtained. For finite values of m_1, $\Delta = 0$ yields the Rician Shadowed model [16], which was shown in [17] that it contains the Hoyt (Nakagami-q) model for $m_1 = 0.5$, with $q = \left(\sqrt{1+2K}\right)^{-1}$. The Rayleigh fading model can be obtained as a particularization of either the aforementioned Rice or Hoyt models for $K = 0$, and also for $m_1 = 1$ and $\Delta = 0$. If there is only one specular component and the diffuse component is absent ($\Delta = 0$, $K \to \infty$), the IFTR model tends to the Nakagami-m model.

III. New Representation of the IFTR Fading Model

In this paper, we present a new statistical characterization of the SNR of a signal undergoing IFTR fading which, denoting by E_s the symbol energy density and N_0 the noise power spectral density, is defined as $\gamma \triangleq (E_s/N_0)\,|V_r|^2$.

Definition 2: A RV γ following an IFTR distribution with parameters m_1, m_2, K, Δ and mean $\bar{\gamma}$ will be denoted by $\gamma \sim \mathcal{IFTR}(\bar{\gamma}, m_1, m_2, K, \Delta)$, and its PDF and CDF will be denoted, respectively, by $f_\gamma^{\mathrm{IFTR}}(\cdot)$ and $F_\gamma^{\mathrm{IFTR}}(\cdot)$.

Following the same spirit as in [18] for TWDP and in [9] and [10] for FTR fading, we now show that the PDF and CDF of the SNR of a RV following an IFTR distribution can be expressed as infinite countable mixtures of the corresponding functions for the Gamma distribution. Additionally, we show how this result can be applied to readily obtain any metric, defined by averaging over the channel realizations, for the IFTR model, from such metric for the much simpler and widely used Nakagami-m fading.

A. PDF and CDF of IFTR Fading

Lemma 1: Let $\gamma \sim \mathcal{IFTR}(\bar{\gamma}, m_1, m_2, K, \Delta)$, then, its PDF and CDF can be expressed, respectively, as

$$f_\gamma^{\mathrm{IFTR}}(x) = \sum_{j=0}^{\infty} A_j f^{\mathcal{G}}\left(x; j+1, \frac{\bar{\gamma}}{1+K}\right), \tag{8}$$

$$F_\gamma^{\mathrm{IFTR}}(x) = \sum_{j=0}^{\infty} A_j F^{\mathcal{G}}\left(x; j+1, \frac{\bar{\gamma}}{1+K}\right), \tag{9}$$

where $f^{\mathcal{G}}$ and $F^{\mathcal{G}}$ are, respectively, the PDF and CDF of the Gamma distribution given in (1) and (2), and coefficients A_j are given in (11), shown at the bottom of the next page, in terms of the channel parameters and the regularized Gauss hypergeometric function,[1] which is defined as

$${}_2\tilde{F}_1(a,b;c;z) = \sum_{k=0}^{\infty} \frac{(a)_k\,(b)_k}{\Gamma(c+k)}\frac{z^k}{k!}, \tag{10}$$

where $(a)_k \triangleq \Gamma(a+k)/\Gamma(a)$ is the Pochhammer symbol.

Proof: See Appendix A. ∎

Note that, in contrast to the PDF and CDF expressions given in [7], (8) and (9) are valid for arbitrary values of m_1 and m_2, and therefore this is also true for all the performance metrics derived from them.

Remark 2: By noting that the j-th term in (8) is proportional to $(x/\bar{\gamma})^j$, the PDF and CDF in IFTR fading in the high SNR regime (i.e., as $\bar{\gamma} \to \infty$) can be approximated by only maintaining the first term in the infinite summations, yielding

$$f_\gamma^{\mathrm{IFTR}}(x) \approx A_0 \frac{1+K}{\bar{\gamma}} e^{-x(1+K)/\bar{\gamma}}, \qquad \bar{\gamma} \gg x, \tag{12}$$

$$F_\gamma^{\mathrm{IFTR}}(x) \approx A_0 \left(1 - e^{-x(1+K)/\bar{\gamma}}\right), \qquad \bar{\gamma} \gg x \tag{13}$$

with

$$A_0 = \frac{m_1^{m_1} m_2^{m_2}}{(K_1+m_1)^{m_1}(K_2+m_2)^{m_2}} \times {}_2F_1\left(m_1, m_2; 1; \frac{K^2\Delta^2}{4(K_1+m_1)(K_2+m_2)}\right). \tag{14}$$

Thus, when averaging over metrics which are fast decreasing on the instantaneous SNR, e.g., bit/symbol error rates, considering only the first term in the resulting summation yields a tight asymptotic result as $\bar{\gamma} \to \infty$.

Corollary 1: Let $h(\gamma)$ be a performance metric (or statistical function) depending on the instantaneous SNR, and let $X_{\mathcal{K}}(\bar{\gamma}_{\mathcal{K}}, m)$ be the metric (or function) obtained by averaging over an interval of the PDF of the SNR for Nakagami-m fading with mean $\bar{\gamma}_{\mathcal{K}}$ and fading severity m, i.e.,

$$X^{\mathcal{K}}(\bar{\gamma}_{\mathcal{K}}, m) = \int_a^b h(x) f^{\mathcal{G}}(x; m, \bar{\gamma}_{\mathcal{K}}/m)dx, \tag{15}$$

[1] The regularized Gauss hypergeometric function can be calculated in terms of the *standard* Gauss hypergeometric function as ${}_2\tilde{F}_1(a,b;c;z) = {}_2F_1(a,b;c;z)/\Gamma(c)$ when $c \notin \{0,-1,-2,\ldots\}$, however, the corresponding parameter c in the coefficients A_j in (11) can indeed be a non-positive integer for some values of index j, therefore, ${}_2\tilde{F}_1$ has to be calculated using (10). Nevertheless, the regularized Gauss hypergeometric function is in-built in the Mathematica software.

where $0 \leq a \leq b \leq \infty$. Then, the average performance metric for IFTR fading can be calculated as

$$X^{\mathrm{IFTR}}(\bar{\gamma}, m_1, m_2, K, \Delta) = \sum_{j=0}^{\infty} A_j X^{\mathcal{K}}\left(\frac{\bar{\gamma}}{1+K}(j+1), j+1\right), \tag{16}$$

where A_j are the IFTR coefficients defined in (11).

Proof: The average metric in IFTR fading channel is calculated as

$$X^{\mathrm{IFTR}}(\bar{\gamma}, m_1, m_2, K, \Delta) = \int_a^b h(x) f_\gamma^{\mathrm{IFTR}}(x)\, dx. \tag{17}$$

By plugging (8) into (17) we can write

$$\begin{aligned} X^{\mathrm{IFTR}}&(\bar{\gamma}, m_1, m_2, K, \Delta) \\ &= \int_a^b h(x) \left[\sum_{j=0}^{\infty} A_j f^{\mathcal{G}}\left(x; j+1, \frac{\bar{\gamma}}{1+K}\right)\right] dx \\ &= \sum_{j=0}^{\infty} A_j \int_a^b h(x) f^{\mathcal{G}}\left(x; j+1, \frac{\bar{\gamma}}{1+K}\right) dx. \end{aligned} \tag{18}$$

Comparing the integral of the resulting expression with (15) and identifying $j+1=m$ and $\frac{\bar{\gamma}}{1+K} = \frac{\bar{\gamma}_{\mathcal{K}}}{m}$, (16) is obtained. ■

B. Series Convergence and Kolmogorov-Smirnov Goodness-of-Fit Statistical Test

The series expression of the PDF given in (8) is calculated by averaging the convergent series for TWDP fading, given in (60), over the fluctuations of the specular components, as explained in Appendix A. The weights of the Gamma PDF's in the TWDP series are positive [18] and therefore the interchange of integration and infinite summation in (61) can be carried out by virtue of Tonelli's theorem [19], which has the following consequences:

(i) The series in the right hand side of (8) converges to the PDF of the IFTR fading model $f_\gamma^{\mathrm{IFTR}}(x)\ \forall x \in [0, \infty)$.

(ii) The calculated coefficients A_j are positive for all j.

Moreover, the performance metrics in communication systems (e.g., BER, channel capacity, outage probability, etc.) are typically non-negative functions which, together with (ii), permits to invoke again Tonelli's theorem, thus allowing the interchange of integration and infinite summation in (18), yielding two additional consequences:

(iii) The series in the right hand side of (16) converges to the average metric in IFTR fading $X^{\mathrm{IFTR}}(\bar{\gamma}, m_1, m_2, K, \Delta)$.

TABLE I
KS TEST FOR IFTR CHANNEL WITH DIFFERENT CHANNEL PARAMETERS K, m_1, m_2, Δ

channel parameters	$J=20$	$J=30$	$J=40$
$K=10,\ m_1=8,\ m_2=5,\ \Delta=0.5$	0.0516	0.0017	0.0013
$K=15,\ m_1=8,\ m_2=5,\ \Delta=0.5$	0.2331	0.0465	0.0052
$K=10,\ m_1=8,\ m_2=5,\ \Delta=0.8$	0.0831	0.0055	0.0043
$K=10,\ m_1=8,\ m_2=5,\ \Delta=0.3$	0.0364	0.0008	0.0007
$K=10,\ m_1=15,\ m_2=5,\ \Delta=0.5$	0.0388	0.0011	0.0009

(iv) Considering $h(\gamma)=1$ in $[0,\infty)$ in Corollary 1 yields $\sum_{j=0}^{\infty} A_j = 1$. Adittionally, considering $h(\gamma)=1$ in $[0,x)$ in Corollary 1 provides a formal justification for obtaining (9) by integrating (8) term by term.

The infinite series used in the statistical characterization of IFTR fading must be truncated for numerical computation. We now provide the KS goodness-of-fit statistical test, which permits to check how close a truncated series is to the exact value. The KS test statistic is given by [20]

$$T_{KS} = max|\hat{F}_\gamma^{\mathrm{IFTR}}(x) - F_\gamma^{\mathrm{IFTR}}(x)|, \tag{19}$$

where $F_\gamma^{\mathrm{IFTR}}(x)$ is the exact value of the CDF and $\hat{F}_\gamma^{\mathrm{IFTR}}(x)$ is the approximation of the CDF when the series is truncated to J terms.

Table I reports the KS test for different channel parameters when the truncated series have 20, 30 or 40 terms. It can be seen that the accuracy reaches an acceptable level when the first 40 terms of the series are computed, so the numerical calculations of all the series in this work will consider 40 terms.

Figs. 1 and 2 show the PDF of the SNR for different IFTR channel parameters obtained from (8) assuming 40 terms in the truncated series computation. Fig. 1 is plotted for $K=12$, $\Delta=0.9$ and different non-integer values of m_1 and m_2, while Fig. 2 shows the PDF for different values of K and Δ with $m_1=30, m_2=25$. The numerical results are verified by Monte-Carlo simulation, showing an excellent agreement in all cases. These results show the great versatility of the IFTR model, as varying the channel parameters results in very different shapes of the PDF. Fig. 3 illustrates the CDF of the SNR in IFTR fading computed from (9) for different values of K, Δ and m_1, m_2. A smoother shape of the CDF indicates a higher variance and therefore an increased probability of experiencing a deep fade. In all these figures it is assumed $\bar{\gamma}=1$.

$$\begin{aligned} A_j = &\sum_{k=0}^{j}\binom{j}{k}\sum_{q=0}^{j-k}\binom{j-k}{q}\frac{K_1^q K_2^{j-k-q}}{j!}\sum_{l=0}^{k}\binom{k}{l}\frac{m_1^{m_1}}{\Gamma(m_1)}\frac{m_2^{m_2}}{\Gamma(m_2)}\frac{\Gamma(m_1+q+l)}{(K_1+m_1)^{m_1+q+l}}\frac{\Gamma(m_2+j-k-q+l)}{(K_2+m_2)^{m_2+j-k-q+l}} \\ &\times(-1)^k\left(\frac{K\Delta}{2}\right)^{2l}{}_2\tilde{F}_1\left(m_1+q+l, m_2+j-k-q+l, 2l-k+1, \frac{K^2\Delta^2}{4(K_1+m_1)(K_2+m_2)}\right). \end{aligned} \tag{11}$$

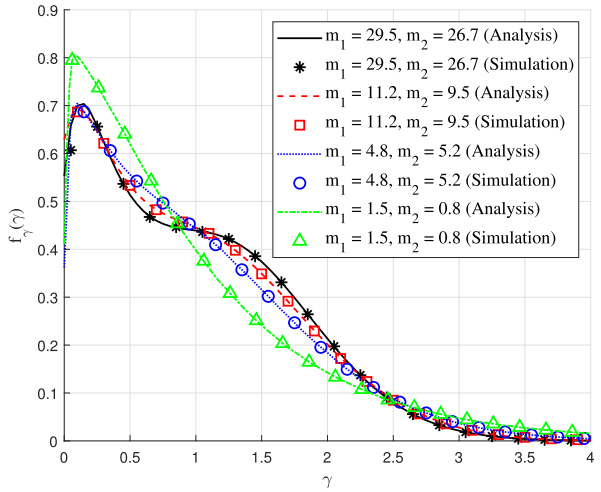

Fig. 1. PDF of the SNR under IFTR fading for different channel parameters m_1, m_2 with $K = 12$ and $\Delta = 0.9$. Simulation confirmation results are displayed as circular markers. $K = 10$. $\bar{\gamma} = 1$.

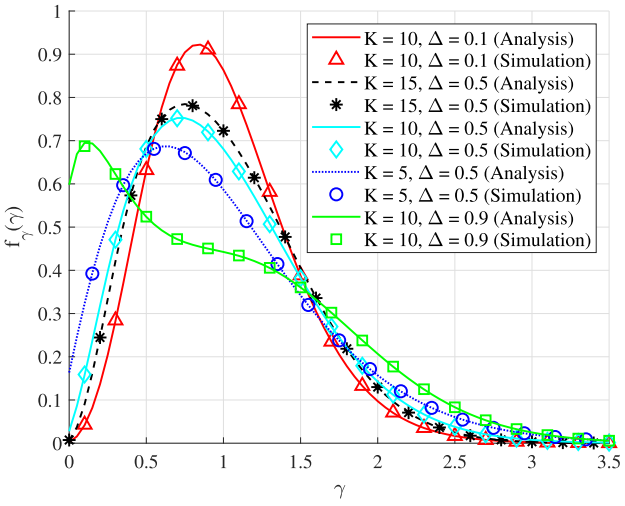

Fig. 2. PDF of the SNR under IFTR fading for different channel parameters K and Δ with $m_1 = 30, m_2 = 25$. Simulation confirmation results are displayed as markers. $\Delta = 0.5$. $\bar{\gamma} = 1$.

C. Empirical Validation

We now show that the new IFTR formulation improves channel fitting to experimental measurements with respect to the original formulation, and also the suitability of the IFTR distribution for modeling small-scale fading in high-frequencies wireless links. We use the empirical measurements results presented in [21] obtained in Brooklyn, New York, where directional horn antennas were used at the transmitter and receiver in a vertical-to-horizontal cross-polarized antenna scenario at the 28 GHz band. We will consider an error factor, ϵ, motivated by the KS statistic, which measures the degree of agreement between the empirical and theoretical CDFs, denoted $F_{emp}(x)$ and $F_{th}(x)$, respectively, as

$$\epsilon \triangleq \max_x |\log_{10}(F_{emp}(x)) - \log_{10}(F_{th}(x))|, \qquad (20)$$

where the logarithm permits to emphasize discrepancies between the CDFs near zero, as certain critical performance metrics in communication systems, such as BER and outage probability, depend on the likelihood of deep fading occurrences.

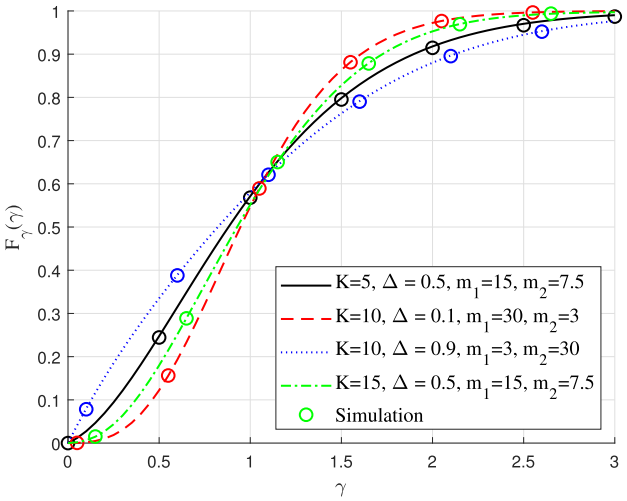

Fig. 3. CDF of the SNR under IFTR fading for different channel parameters m_1, m_2, K, and Δ. Simulation confirmation results are displayed as circular markers. $\bar{\gamma} = 1$.

TABLE II
FITTING RESULTS AT 28 GHZ

channel model	ϵ	Δ	K	$m_1, m_2/m$
New IFTR	0.2170	0.8487	467.5652	9.2,50.6
Original IFTR [8]	0.2203	0.8463	476.1454	9,50.5
FTR [9]	0.2246	0.5873	80.3916	2

The parameters of the IFTR distribution, m_1, m_2, K, and Δ have been optimized from the CDF of the experimental data set at $x = r^2/\mathbb{E}\{r^2\}$, where $r = |V_r|$ represents the signal envelope. We illustrate in Table II the optimal parameter values of both the original and the new IFTR formulation proposed here, which shows that the new one can achieve a lower error by using non-integer values of all channel parameters. In addition, the FTR model results are also presented, which is shown to provide a worse match to the considered empirical data than the IFTR model.

D. GMGF and Moments of the IFTR Model

Definition 3: Let $n > 0$, and let X be a continuous non-negative RV with PDF $f_X(\cdot)$. The GMGF of X is defined as

$$\phi_X^{(n)}(s) \triangleq E\left\{X^n e^{Xs}\right\} = \int_0^\infty x^n e^{xs} f_X(x)\, dx, \qquad (21)$$

where $E\{\cdot\}$ denotes the expectation operator. The moment generating function (MGF) is defined as $\phi_X(s) \triangleq E\left\{e^{Xs}\right\} = \phi_X^{(0)}(s)$, and it is therefore a particular case of the GMGF. Note that for $n \in \mathbb{N}$, the GMGF coincides with the n-th order derivative of the MGF. Also, the n-th order moment of X is obtained as $E\{X^n\} = \phi_X^{(n)}(0)$.

The GMGF finds application in different communication theory areas, including energy detection, outage probability under co-channel interference, physical layer security or BER analysis. In most cases it suffices to consider $n \in \mathbb{N}$, which usually results in closed-form expressions for the GMGF, such

as it is the case for IFTR fading, as we show bellow. However, there are situations, such as composite Inverse Gamma (IG) shadowing/fading modeling [22], where the more general case of arbitrary $n > 0$ needs to be considered. In the following Lemma we derive expressions for the GMGF of the IFTR fading model for both cases.

Lemma 2: Let $\gamma \sim \mathcal{IFTR}(\overline{\gamma}, m_1, m_2, K, \Delta)$, then, its GMGF can be expressed as follows:

(i) General case ($n \in \mathbb{R}^+$):

$$\phi_{\gamma}^{(n)}(s) = \sum_{j=0}^{\infty} A_j \phi_G^{(n)} \left(s, j+1, \frac{\bar{\gamma}}{1+K} \right), \tag{22}$$

where A_j is defined in (11) and $\phi_G^{(n)}$ is the GMGF of a RV $G \sim \mathcal{G}(\lambda, \nu)$, which is given by

$$\phi_G^{(n)}(s, \lambda, \nu) = \frac{\Gamma(n+\lambda)\left(\frac{1}{\nu} - s\right)^{-(n+\lambda)}}{\Gamma(\lambda)\nu^{\lambda}}. \tag{23}$$

(ii) Case $n \in \mathbb{N}$: A closed-form expression is given in (24), shown at the bottom of the next page.

Proof:

Case (i): This result is obtained by by applying Corollary 1 to the GMGF of the SNR in Nakagami-m fading given in [22, Table II].

Case (ii): See Appendix B. ∎

Lemma 3: Let $\gamma \sim \mathcal{IFTR}(\overline{\gamma}, m_1, m_2, K, \Delta)$, then its n-th order moment can be expressed as follows:

(i) General case ($n \in \mathbb{R}^+$):

$$E\{\gamma^n\} = \sum_{j=0}^{\infty} A_j \frac{\Gamma(n+j+1)\bar{\gamma}^n}{\Gamma(j+1)(1+K)^n}. \tag{25}$$

(ii) Case $n \in \mathbb{N}$: A closed-form expression is given now by

$$\begin{aligned} E\{\gamma^n\} = & \left(\frac{\overline{\gamma}}{1+K}\right)^n \sum_{q=0}^{n} \binom{n}{q} \frac{n!}{q!} \sum_{r=0}^{q} \binom{q}{r} \\ & \times \sum_{p=0}^{q-r} \binom{q-r}{p} K_1^p K_2^{q-r-p} \sum_{l=0}^{r} \binom{r}{l} \left(\frac{K\Delta}{2}\right)^{2l} \\ & \times \frac{\Gamma(m_1+l+p)}{\Gamma(m_1) m_1^{l+p}} \frac{\Gamma(m_2+q-l-p)}{\Gamma(m_2) m_2^{q-l-p}} \delta_{2l,r}. \end{aligned} \tag{26}$$

where $\delta_{2l,r}$ is the kronecker delta function.

Proof: These results follows by considering $s = 0$ in the GMGF expressions. In case (ii), the following equality has been taken into account to obtain (26):

$$\lim_{s \to 0} s^{n-m} \cdot {}_2\tilde{F}_1\left(a, b; n-m+1; A \cdot s^2\right) = \delta_{n,m}, \tag{27}$$

which holds for any $n, m \in \mathbb{N}$, where the cases $n > m$ and $n = m$ are trivial, and the case $n < m$ results from the fact that the Gamma function has simple poles at the non-positive integers, and therefore from (10) and given $p \in \mathbb{N} \cup \{0\}$ we can write

$${}_2\tilde{F}_1(a, b; -p; z) = \sum_{k=p+1}^{\infty} \frac{(a)_k (b)_k}{\Gamma(-p+k)} \frac{z^k}{k!}. \tag{28}$$

∎

From the expression of the moments for $n \in \mathbb{N}$ given in (26), a closed-form expression for the amount of fading (AoF) for IFTR fading can be obtained in closed-form. The AoF captures the severity, in terms of the variability, of the fading channel as a function of the parameters of the model and is defined as the variance of the SNR normalized by its squared mean, so that AoF $\triangleq E\{(\gamma - \bar{\gamma})^2\}/\bar{\gamma}^2 = E\{\gamma^2\}/\bar{\gamma}^2 - 1$.

Corollary 2: Let $\gamma \sim \mathcal{IFTR}(\overline{\gamma}, m_1, m_2, K, \Delta)$, then, its AoF can be written as

$$\text{AoF} = \frac{1}{(1+K)^2}\left[1 + 2K + \frac{(K\Delta)^2}{2} + \frac{K_1^2}{m_1} + \frac{K_2^2}{m_2}\right]. \tag{29}$$

Proof: This result is obtained by particularizing the moments in (26) to the definition of the AoF. ∎

The IFTR fading model tends to the TWDP one for $m_1, m_2 \to \infty$. As a check, it must be noted that for such condition the expression given in (29) tends to the AoF given in [23, eq. (34)] for TWDP fading.

IV. Performance Analysis

By using the derived statistical characterization of the IFTR fading model, the performance of different wireless communication systems undergoing this fading distribution can be calculated. In the following, the channel capacity, the ergodic mutual information for discrete inputs, the outage probability in a noise-limited and in an interference-limited multi-antenna receiver, the secrecy capacity outage probability and the bit error rate for different modulations have been obtained for IFTR fading.

A. Average Channel Capacity

The average capacity per unit bandwidth for IFTR fading is given by

$$\bar{C} = \int_0^{\infty} \log_2(1+x) f_{\gamma}^{\text{IFTR}}(x) dx. \tag{30}$$

A direct application of Corollary I using the average channel capacity expression for Nakagami-m fading channels [24, eq. (23)] provides the following closed-form expression:

$$\bar{C} = \sum_{j=0}^{\infty} \frac{A_j e^{\frac{K+1}{\bar{\gamma}}}}{\ln(2)} \sum_{k=0}^{j} \left(\frac{1+K}{\bar{\gamma}}\right)^k \Gamma\left(-k, \frac{1+K}{\bar{\gamma}}\right), \tag{31}$$

where A_j is given in eq. (11) and $\Gamma(.,.)$ is the upper incomplete gamma function, which can be computed, when the first parameter is a negative integer, as [14, eq. (8.352.3)]

$$\Gamma(-n, x) = \frac{(-1)^n}{\Gamma(n)}\left[\sum_{r=0}^{n-1} \frac{\Gamma(n-r)}{(-x)^{n-r} e^x} - Ei(-x)\right], \tag{32}$$

where $Ei(\cdot)$ is the exponential integral function [14, eq. (8.211.1)].

The asymptotic channel capacity in the high SNR regime ($\bar{\gamma} \to \infty$) can be expressed as [25]

$$\bar{C} \approx \log_2(e)\left(\ln \overline{\gamma} + \mu\right), \tag{33}$$

where $\mu < 0$ represents the capacity loss due to fading with respect to the AWGN case (for which $\mu = 0$), and can be calculated in terms of the derivative of the moments of the fading distribution as

$$\mu = \frac{1}{\overline{\gamma}^n} \frac{\partial}{\partial n} E\left\{\gamma^n\right\}. \tag{34}$$

In the case of Nakagami-m fading for $m \in \mathbb{N}$, the value of μ is given by $\mu_{\text{Nak}} = H_{m-1} - \gamma_e - \ln(m)$ [25, eq. (21b)], where $H_n \triangleq \sum_{k=1}^{n} (1/k)$ is the n-th harmonic number and γ_e is the Euler-Mascheroni constant [26, eq. (6.1.3)]. From Corollary I, the asymptotic channel capacity for IFTR fading can thus be written as

$$\bar{C} \approx \log_2(e) \cdot \left[\ln\left(\frac{\overline{\gamma}}{1+K}\right) - \gamma_e + \sum_{j=1}^{\infty} A_j H_j \right]. \tag{35}$$

B. Ergodic Mutual Information

Let us assume the scalar AWGN channel with output $Y = \sqrt{\gamma} X + N$, where $N \sim \mathcal{CN}(0,1)$ represents the complex Gaussian noise, γ represents a particular realization of the channel power gain, and X is the input signal, with $E\{|X|^2\} = 1$, taking values with some given probabilities from the constellation alphabet $\mathcal{X}$. When $\mathcal{X}$ is a Gaussian constellation, the instantaneous input-output mutual information is given by $\mathcal{I}(\gamma) = \log_2(1+\gamma)$, and in this case the ergodic mutual information, which is obtained by promediating $\mathcal{I}(\gamma)$ over the realizations of γ, is actually the average channel capacity defined in (30).

However, in practical communication systems, $\mathcal{X}$ is a finite set. In this subsection we will consider that $\mathcal{X}$ is an M-QAM constellation with equal-probability symbols. In this case, $\mathcal{I}(\gamma)$ is given in [27, eq. (5)], but it is not expressed in closed-form, and the problem of finding the exact ergodic mutual information becomes intractable. However, it is demonstrated in [27, eq. (26)] that a tight and general approximated closed-form expression of the ergodic mutual information is given by

$$\bar{\mathcal{I}} \approx \log_2 M \times \left(1 - \sum_{i=1}^{k_M} \zeta_i^{(M)} \phi_\gamma\left(-\vartheta_i^{(M)}\right)\right), \tag{36}$$

where k_M, $\zeta_i^{(M)}$ and $\vartheta_i^{(M)}$ are constants which are given in [27, Table I], and $\phi_\gamma(\cdot)$ is the MGF of the fading model, which is given in (24) for the case when $n = 0$ for IFTR fading. Thus, for this channel model, the ergodic mutual information can be written as in (37), shown at the bottom of the next page, from which a simpler asymptotic expression in the high SNR regime can be found to be given as

$$\begin{aligned} \bar{\mathcal{I}} &\approx \log_2 M \\ &\times \left(1 - \sum_{i=1}^{k_M} \zeta_i^{(M)} \frac{1+K}{\bar{\gamma}\vartheta_i^{(M)}} \frac{m_1^{m_1}}{(m_1+K_1)^{m_1}} \frac{m_2^{m_2}}{(m_2+K_2)^{m_2}} \right. \\ &\left. \times {}_2F_1\left(m_1, m_2; 1; \frac{(K\Delta)^2}{4(m_1+K_1)(m_2+K_2)}\right)\right), \\ &\bar{\gamma} \to \infty. \end{aligned} \tag{38}$$

C. Outage Probability

1) Noise-Limited Reception: The outage probability, i.e., the probability that the received SNR is below a threshold γ_{th}, under IFTR fading is given by

$$P_{out} = Pr(\gamma < \gamma_{th}) = F_\gamma^{\text{IFTR}}(\gamma_{th}), \tag{39}$$

where $F_\gamma^{\text{IFTR}}(\cdot)$ is given in (9). An asymptotic outage probability expression in the high SNR regime can be obtained from (13), or alternatively, by considering in this expression the approximation $e^x \approx 1 + x$ for $|x| \ll 1$, it can be written as

$$P_{out} \approx A_0 \frac{1+K}{\bar{\gamma}} \gamma_{th}, \quad \bar{\gamma} \to \infty. \tag{40}$$

2) Interference-Limited Multi-Antenna Reception: In the presence of co-channel interference (CCI) of total received power I, considering negligible background noise and denoting as W the received power from the desired user, which is assumed to experience IFTR fading, the outage probability is defined as

$$\hat{P}_{\text{out}} = P\left(\frac{W}{I} < R_{th}\right), \tag{41}$$

where R_{th} denotes the signal-to-interference (SIR) threshold.

We further assume N receive antennas performing maximal ratio combining (MRC) and L independent and identically distributed (i.i.d.) Rayleigh interferers with average power P_I. We denote as W_i the desired user power at antenna i. In this scenario, the outage probability is given by [28, eq. (15)]

$$\hat{P}_{\text{out}} = \sum_{k=0}^{L-1} \left(\frac{1}{R_{th} P_I}\right)^k \sum_{\mathcal{U}} \prod_{i=1}^{N} \frac{1}{u_i!} \phi_{W_i}^{(u_i)}\left(-\frac{1}{R_{th} P_I}\right), \tag{42}$$

$$\begin{aligned} \phi_\gamma^{(n)}(s) = {} & \frac{\overline{\gamma}^n n!}{(1+K-\bar{\gamma}s)^{n+1-m_1-m_2}} \frac{m_1^{m_1}}{\Gamma(m_1)} \frac{m_2^{m_2}}{\Gamma(m_2)} \sum_{q=0}^{n} \binom{n}{q} \frac{(1+K)^{q+1}}{q!} \sum_{r=0}^{q} \binom{q}{r} \sum_{p=0}^{q-r} \binom{q-r}{p} K_1^p K_2^{q-r-p} \\ & \times \sum_{l=0}^{r} \binom{r}{l} \left(\frac{K\Delta}{2}\right)^{2l} \frac{\Gamma(m_1+l+p)}{(m_1(1+K)-(m_1+K_1)\bar{\gamma}s)^{m_1+l+p}} \frac{\Gamma(m_2+l-p+q-r)}{(m_2(1+K)-(m_2+K_2)\bar{\gamma}s)^{m_2+l-p+q-r}} (\bar{\gamma}s)^{2l-r} \\ & \times {}_2\tilde{F}_1\left(m_1+l+p, m_2+l-p+q-r; 2l-r+1; \frac{(K\Delta\bar{\gamma}s)^2}{4(m_1(1+K)-(m_1+K_1)\bar{\gamma}s)(m_2(1+K)-(m_2+K_2)\bar{\gamma}s)}\right). \end{aligned} \tag{24}$$

where $\mathcal{U}$ is a set of N-tuples such that $\mathcal{U} = \{(u_1 \dots u_N), u_i \in \mathbb{N}, \sum_{i=1}^{N} u_i = k\}$. The relation $W_i = \frac{\gamma_i}{E_s/N_0}$ results in $W_i \sim \mathcal{IFTR}(\overline{W}, m_1, m_2, K, \Delta)$, with $\overline{W}$ the average desired user power at every antenna. Therefore, $\phi_{W_i}^{(u_i)}(s)$ is computed using (24), as $u_i \in \mathbb{N}$, by simply substituting $\bar{\gamma}$ by $\overline{W}$, thereby providing a closed-form expression for the outage probability.

An asymptotic expression of the outage probability for $(\overline{W}/P_I) \gg R_{th}$ can be expressed as

$$\hat{P}_{out} \approx Q \cdot \left[\frac{R_{th}\,(1+K)}{\overline{W}/P_I} \frac{m_1^{m_1}}{(m_1+K_1)^{m_1}} \frac{m_2^{m_2}}{(m_2+K_2)^{m_2}} \times {}_2\overline{F}_1\left(m_1, m_2; 1; \frac{(K\Delta)^2}{4\,(m_1+K_1)\,(m_2+K_2)}\right)\right]^N, \tag{43}$$

where $Q = \sum_{k=0}^{L-1} S(k,N)$, and where $S(k,N)$ is the number of elements of set $\mathcal{U}$ (i.e., the number N-partitions of integer k), which can be calculates recursively as $S(k,N) = S(k-1,N) + S(k,N-1)$, with $S(1,N) = N, S(0,N) = 1, S(k,1) = 1$ [28, Appendix II]. It is interesting to note that the outage probability given in (43) is inversely proportional to the N-th power of $\overline{W}/P_I$ due to the MRC reception.

D. Average BER

The average bit/symbol error rate in a telecommunication system is one of the main parameters for measuring the quality of communication. In this section, we calculate this metric for the IFTR fading channel. The conditional BER probability in an AWGN channel for some relevant modulations with coherent detection can be written as [29]

$$P_e(x) = \sum_{r=1}^{R} \alpha_r Q(\sqrt{\beta_r x}). \tag{44}$$

The average BER is calculated by averaging (44) over all possible channel realizations. From the result in [30, eq. (5.18)] for Nakagami-m fading, by virtue of Corollary 1, the average BER in IFTR fading can be written, after some manipulation, as

$$\bar{P}_e = \sum_{r=1}^{R} \frac{\alpha_r}{2} \sum_{j=0}^{\infty} A_j \left[1 - \sqrt{\frac{\beta_r\overline{\gamma}}{2\,(1+K)+\beta_r\overline{\gamma}}} \sum_{k=0}^{j} \binom{2k}{k} \times \left(\frac{1-\frac{\beta_r\overline{\gamma}}{2(1+K)+\beta_r\overline{\gamma}}}{4}\right)^k\right]. \tag{45}$$

In the high SNR regime, the average BER can be simplified by simply maintaining the first term in the infinite summation, as stated in Remark 2, yielding

$$\bar{P}_e \approx \sum_{r=1}^{R} \frac{\alpha_r}{2} A_0 \left[1 - \sqrt{\frac{\beta_r\overline{\gamma}}{2\,(1+K)+\beta_r\overline{\gamma}}}\right],\ \bar{\gamma} \to \infty. \tag{46}$$

Asymptotic expressions of symbol error rates are more typically given in terms of a power of $\bar{\gamma}$. We can obtain such result from (46) by considering the approximation $0.5\left(1-\sqrt{x/(1+x)}\right) \approx 1/(4x)$ when $x \gg 1$ [31]. Thus, we can write

$$\bar{P}_e \approx \frac{1+K}{2\bar{\gamma}} A_0 \sum_{r=1}^{R} \frac{\alpha_r}{\beta_r},\quad \bar{\gamma} \to \infty, \tag{47}$$

which, as expected, coincides with the asymptotic expression in [7, eq. (15)] and reveals that the diversity gain of the IFTR model is always 1 for single antenna reception.

E. Secrecy Capacity Outage Probability

We consider that two legitimate peers, Alice (transmitter) and Bob (receiver), want to communicate over a wireless link in the presence of an eavesdropper (Eve). Let us denote as γ_b the instantaneous SNR at the receiver for the link between Alice and Bob, and γ_e the instantaneous SNR at the eavesdropper for the eavesdropping link between Alice and Eve.

The normalized secrecy capacity is defined as [32] $C_s = \max\{\log(1+\gamma_b) - \log(1+\gamma_e), 0\}$. By denoting R_s as the threshold rate under which secure communication cannot be achieved, the secrecy capacity outage probability is defined as $P(C_s < R_s) = 1 - P(C_s > R_s)$, where $P(C_s > R_s)$ is the probability of achieving a successful secure communication between Alice and Bob, which can be written as [33, eq. (9)]

$$P(C_s > R_s) = \int_0^{\infty} f_{\gamma_e}(x)\left(1 - F_{\gamma_b}(2^{R_s}(1+x)-1)\right)dx, \tag{48}$$

where $f_{\gamma_e}(\cdot)$ is the PDF of γ_e, which is assumed to follow an arbitrary distribution. On the other hand, the legitimate channel is assumed to undergo IFTR fading, and therefore $F_{\gamma_b}(\cdot)$,

$$\bar{\mathcal{I}} \approx \log_2 M \times \left(1 - \sum_{i=1}^{k_M} \zeta_i^{(M)} \frac{1+K}{1+K+\bar{\gamma}\vartheta_i^{(M)}} \frac{m_1^{m_1}}{\left(m_1 + K_1 \frac{\bar{\gamma}\vartheta_i^{(M)}}{1+K+\bar{\gamma}\vartheta_i^{(M)}}\right)^{m_1}} \frac{m_2^{m_2}}{\left(m_2 + K_2 \frac{\bar{\gamma}\vartheta_i^{(M)}}{1+K+\bar{\gamma}\vartheta_i^{(M)}}\right)^{m_2}} \times {}_2F_1\left(m_1, m_2; 1; \frac{\left(K\Delta\bar{\gamma}\vartheta_i^{(M)}\right)^2}{4\left(m_1\,(1+K) + (m_1+K_1)\,\bar{\gamma}\vartheta_i^{(M)}\right)\left(m_2\,(1+K) + (m_2+K_2)\,\bar{\gamma}\vartheta_i^{(M)}\right)}\right)\right). \tag{37}$$

which represents the CDF of γ_b, is given in (9). Leveraging on the closed-form expression of the probability of successful secure transmission given in [34, eq. (34)] when the legitimate link undergoes Nakagami-m, by virtue of Corollary I, when this link experience IFTR fading we can write

$$P(C_s > R_s) = \sum_{j=0}^{\infty} A_{j,b} e^{\frac{1+K}{\bar{\gamma}_b}(1-2^{R_s})} \sum_{p=0}^{j} \frac{1}{p!} \left(\frac{1+K}{\bar{\gamma}_b}\right)^p \times \sum_{n=0}^{p} \binom{p}{n} 2^{nR_s} (2^{R_s}-1)^{p-n} \phi_{\gamma_e}^{(n)} \left(-2^{R_s}\frac{1+K}{\bar{\gamma}_b}\right), \tag{49}$$

where $A_{j,b}$ refer to the coefficients of the channel at Bob. Note that this result is valid for an arbitrary fading distribution of the eavesdropper link, as long as its GMGF is known. The GMGF of different classical and generalized fading models can be found in [22, Table II]. When the eavesdropper link undergoes IFTR fading, (24) is used in (49).

An asymptotic expression for the successful secure communication (and therefore, for the secrecy outage probability) in the high SNR regime of the legitimate channel can be obtained by introducing (13) into (48) to approximate $F_{\gamma_b}(\cdot)$, yielding

$$\begin{aligned} P(C_s > R_s) &\approx 1 - A_{0,b} \times \int_0^{\infty} f_{\gamma_e}(x) \left(1 - e^{-\frac{1+K_b}{\bar{\gamma}_b}(2^{R_s}+2^{R_s}x-1)}\right) dx \\ &\approx 1 - A_{0,b} \times \int_0^{\infty} f_{\gamma_e}(x) \left(\frac{1+K_b}{\bar{\gamma}_b}(2^{R_s}+2^{R_s}x-1)\right) dx, \quad \bar{\gamma}_b \to \infty. \end{aligned} \tag{50}$$

By noticing that $\int_0^{\infty} f_{\gamma_e}(x)x dx = \bar{\gamma}_e$, we finally obtain

$$P(C_s > R_s) \approx 1 - A_{0,b}\frac{1+K_b}{\bar{\gamma}_b}\left(2^{R_s}\bar{\gamma}_e + 2^{R_s} - 1\right), \quad \bar{\gamma}_b \to \infty. \tag{51}$$

It is interesting to note that, in the high SNR regime, the distribution of γ_b dominates the secrecy outage probability, which does not depend on the fading parameters of the eavesdropper channel, but only on its average value $\bar{\gamma}_e$.

V. Numerical and Simulation Results

This section presents figures illustrating the performance of IFTR fading channels. The obtained numerical results have been validated by Monte Carlo simulations, where 10^7 random realizations of the IFTR distribution have been computed. Based on Table I, numerical results involving infinite series have been calculated truncating to 40 terms, as it provides a satisfactory accuracy for all the considered cases.

The average channel capacity for IFTR fading is presented in Figs. 4 and 5 for different values of the channel parameters $\{m_1, m_2, K, \Delta\}$. The presented exact and asymptotic (in Fig. 5) numerical results have been obtained from (31) and (35), respectively. In Fig. 4 it can be seen that a higher

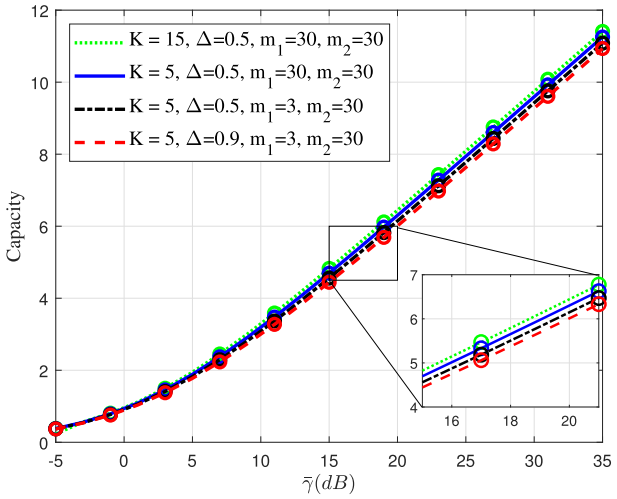

Fig. 4. Numerical and simulation results for the average capacity vs. average SNR in dB for different channel parameters values. Simulation confirmation results are displayed as circular markers.

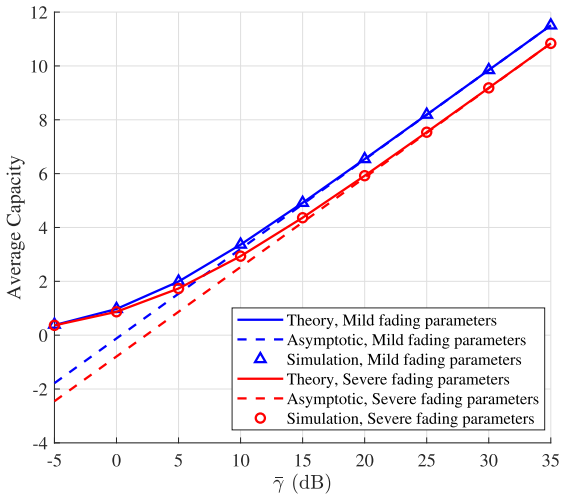

Fig. 5. Numerical, simulation and asymptotic results for the average capacity vs. average SNR in dB for two different groups of channel parameters: mild fading ($K = 15, \Delta = 0.1, m_1 = m_2 = 30$) and severe fading ($K = 1, \Delta = 0.9, m_1 = m_2 = 2.5$).

capacity is obtained for high K. On the other hand, a high value of Δ (close to 1) yields lower capacity due to the increased probability that the specular components cancel each other, which increases the channel variability. Fig. 5 shows that, as expected, a wireless link undergoing severe fading (with parameters $K = 1, \Delta = 0.9, m_1 = m_2 = 2.5$) yields a lower average channel capacity than in the case of mild fading ($K = 15, \Delta = 0.1, m_1 = m_2 = 30$).

Fig. 6 shows the ergodic mutual information as a function of $\bar{\gamma}$ considering different values of M when a discrete M-QAM constellation is used. The figure depicts both the analytical approximate results from (37) as well as exact simulation results, showing a very good agreement. The considered IFTR fading channel parameters correspond to the ones obtained from the empirical measurements used in Section III-C, i.e., $K = 467.5652$, $\Delta = 0.8487$, $m_1 = 9.2$ and $m_2 = 50.6$.

Fig. 7 shows the outage probability (P_{out}), computed from (39) (exact) and (40) (asymptotic), versus the average

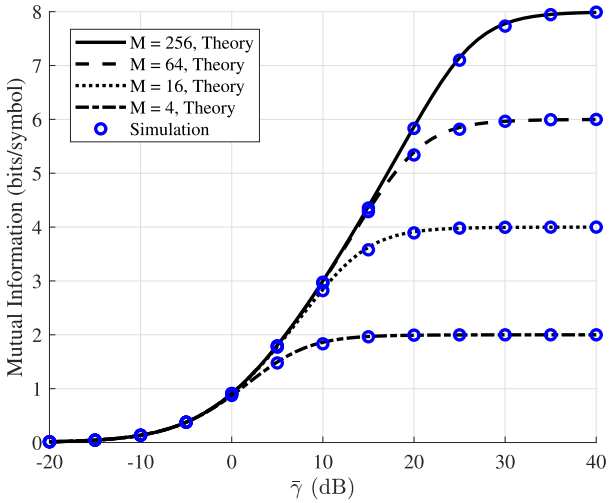

Fig. 6. Analysis approximation and exact simulation results for the ergodic mutual information vs. $\bar{\gamma}$ in dB for M-QAM symbols with channel parameters $K = 467.5652, \Delta = 0.8487, m_1 = 9.2, m_2 = 50.6$.

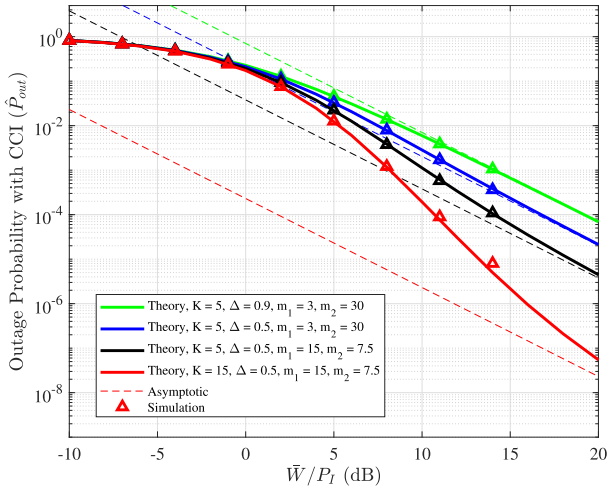

Fig. 8. Numerical, simulation and asymptotic results for the outage probability for IFTR fading with CCI for different channel parameters values with $N = 2$, $L = 1$, and $R_{th} = 0$ dB.

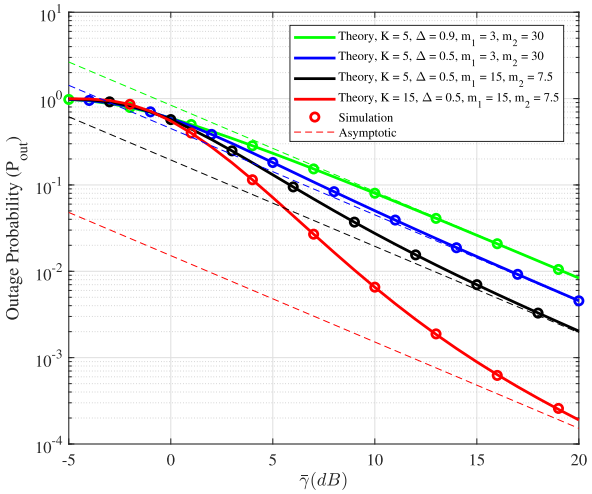

Fig. 7. Numerical, simulation and asymptotic results for the outage probability vs. average SNR in dB.

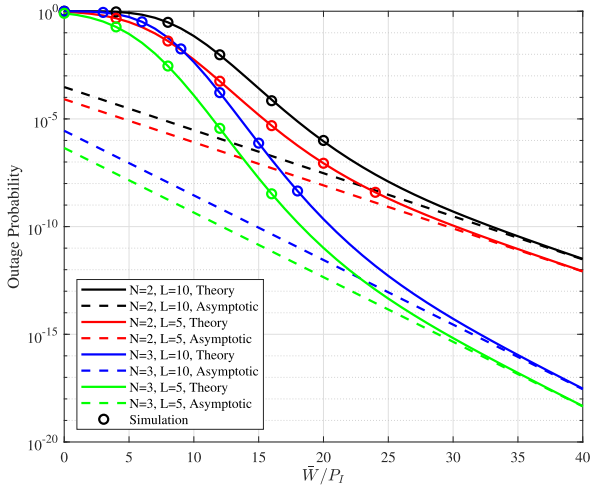

Fig. 9. Numerical, simulation and asymptotic results for the outage probability for IFTR fading with CCI considering different values of the number of antennas $N = 2, 3$ and interferers $L = 5, 10$ with $R_{th} = 1$, $m_1 = 30, m_2 = 3, K = 10$ and $\Delta = 0.1$.

SNR ($\bar{\gamma}$) for different channel model parameters values. It can be observed that decreasing Δ from 0.9 to 0.5, increasing K from 5 to 15, and increasing m_1, when $K = 5$ and $\Delta = 0.5$, yields a better performance (lower outage probability), as these changes give rise to a reduced fading severity.

Figs 8 and 9 show the outage probability considering CCI and multi-antenna MRC reception. The exact and asymptotic results are obtained in this case from (42) and (43), respectively. In Fig. 8 the same values of the IFTR model parameters as in Fig. 7 are considered, and a similar impact of these parameters on performance is observed, although the amount of variation in the outage probability is affected by the presence of interference and multiple antennas. Fig 9 shows how the outage probability improves (decreases) and the number of antennas increases and the number of interferes decreases. It can be seen that the number of antennas has a higher impact, as it affects the slope of the outage probability for high values of $\overline{W}/P_I$. Fig. 10 depicts the outage probability with CCI for different system parameters vs. the SIR threshold considering different values of the number of antennas $N = 1, 2$ and parameter $K = 1, 5, 10, 15$. It is observed that the outage probability increases as the threshold also increases, as expected.

Figs. 11 and 12 show the exact, from (45), simulation and asymptotic, from (47), BER vs. the average SNR in IFTR fading for BPSK modulation ($R = 1$, $\alpha_1 = 1$, $\beta_1 = 2$). In Fig. 11 different values of $\Delta = 0.1, 0.5, 0.9$ are considered when the fading severity parameters, m_1 and m_2 are non-integers. Again, increasing Δ results in higher channel variability, causing a detrimental impact on performance, i.e., a higher average BER. It is worth mentioning that when the average SNR is above 20 dB, the asymptotic curves, which are much simpler to compute, yield very good approximate results, and above 30 dB the exact and asymptotic results are indistinguishable in all the presented cases. In Fig. 12 different values of $K = 1, 5, 15$ are assumed and it can be seen that higher values of K (i.e., higher average power of the specular

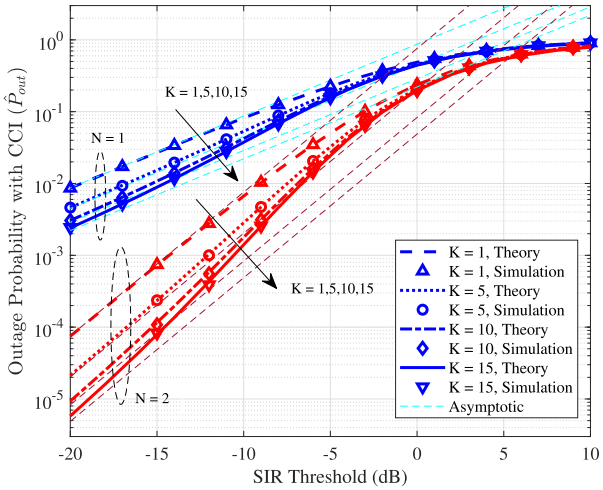

Fig. 10. Numerical, simulation and asymptotic results for the outage probability for IFTR fading with CCI considering different values of $K = 1, 5, 10, 15$ and $N = 1, 2$, with $L = 1$ and $\overline{W}/P_I = 1$. Channel parameters are $m_1 = 3$, $m_2 = 30$ and $\Delta = 0.5$.

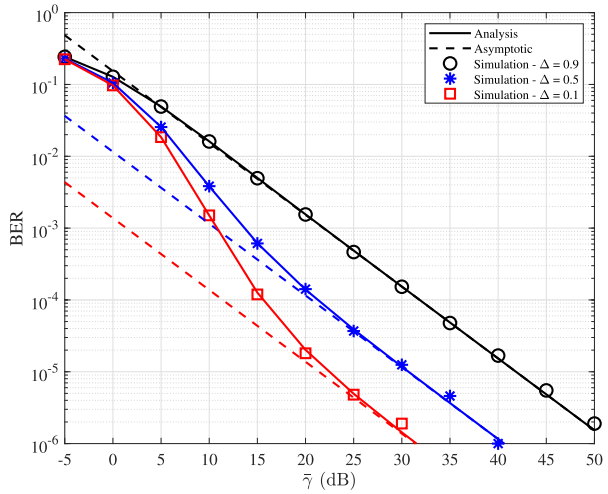

Fig. 11. Numerical, simulation and asymptotic results for the average BER vs. average SNR in dB for BPSK considering different values of Δ with channel parameters $m_1 = 15.7$, $m_2 = 5.1$ and $K = 10$.

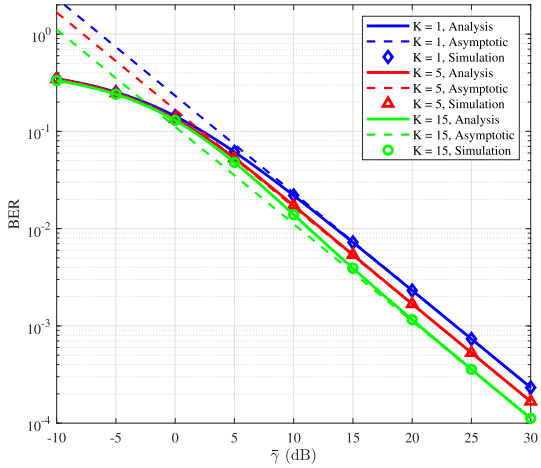

Fig. 12. Numerical, simulation and asymptotic results for the average BER vs. average SNR in dB for BPSK considering different values of K with channel parameters $m_1 = 1.5$, $m_2 = 0.9$ and $\Delta = 1$.

components) improves (decreases) the BER. In this case, the exact and asymptotic results are indistinguishable above 20 dB of the average SNR.

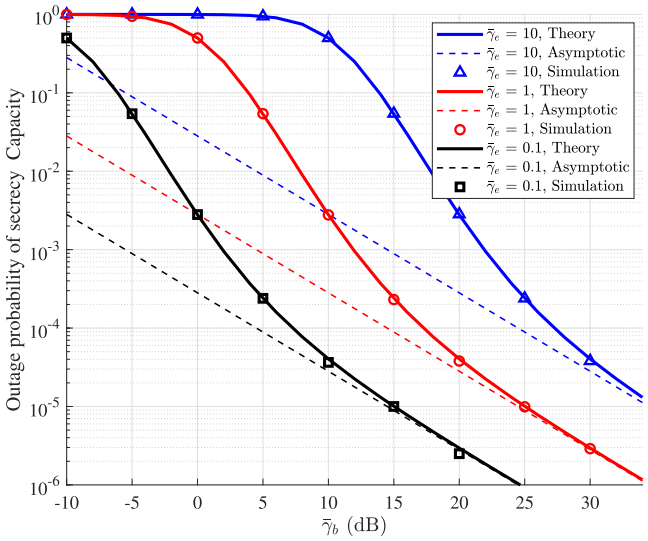

Fig. 13. Outage probability of secrecy capacity vs. average SNR $\bar{\gamma}_b$ in dB for different values of the Eve average SNR $\bar{\gamma}_e$ when both channels undergo IFTR fading with parameters $m_1 = 25.5$, $m_2 = 7.5$, $K = 10$, and $\Delta = 0.1$.

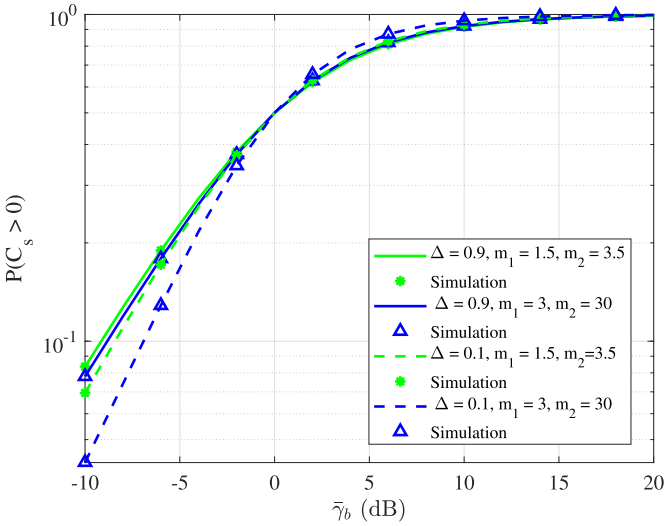

Fig. 14. Probability of strictly positive secrecy capacity as a function of $\bar{\gamma}_b$ in dB for different values of the IFTR channel parameters Δ, m_1, m_2 for both legitimate and eavesdropper IFTR links, with $K = 5$, $\Delta = 0.5$, and $\bar{\gamma}_e = 1$.

Fig. 13 presents the outage probability of secrecy capacity, when both the legitimate and eavesdropper links undergo IFTR fading with average SNR $\bar{\gamma}_b$ and $\bar{\gamma}_e$, respectively, and the remaining parameters (m_1, m_2, K and Δ) are assumed to be the same for both links. A threshold $R_s = 0.1$ is assumed, and the secrecy capacity outage probability is shown as a function of $\bar{\gamma}_b$ and considering different values of $\bar{\gamma}_e$. It can be observed that, by either increasing $\bar{\gamma}_b$ of the legitimate link or decreasing $\bar{\gamma}_e$ of the eavesdropper link, the outage secrecy capacity decreases.

The probability of strictly positive secrecy capacity, defined as $P(C_s > 0)$, is evaluated in Fig. 14 considering IFTR fading for both the legitimate and eavesdropper links for different channel parameter values as a function of $\bar{\gamma}_b$. Two different values of $\Delta = 0.1, 0.9$ are compared for different sets of (m_1, m_2). It is shown that, for low values of $\bar{\gamma}_b$, increasing

the similarity of the two specular components by increasing Δ provides a higher probability of strictly positive secrecy, which is a result of the increased probability of the eavesdropper to experience a deep fade. On the other hand, higher values of m_1 and m_2, which results in milder fluctuations, decreases the secrecy capacity. These results indicate that for lower values of $\bar{\gamma}_b$, the channel parameter values of the eavesdropper link dominates over those of the legitimate link.

VI. Conclusion

In this paper, a new formulation in series form has been derived for the PDF and CDF of the IFTR fading model. The convergence of the obtained series are demonstrated and truncated for numerical computation using the Kolmogorov-Smirnov goodness-of-fit. We show that, leveraging on any average performance metric already known for the much simpler Nakagami-m fading model, such metric can be readily obtained for IFTR fading. Also the new formulation is shown to provide a better match to empirical measurements than the original one, as arbitrary values for the fading parameters are permitted.

Additionally, the GMGF of IFTR fading has been obtained which, for most cases of interest, can be expressed in closed-form, thus opening the door to circumvent the model mathematical complexity and obtain several relevant performance metrics also in closed-form, as well as the moments of the distribution and the amount of fading. Finally, the new and expanded statistical characterization of the IFTR fading model has been exemplified, showing and discussing numerical results and the impact of channel parameter values for the average channel capacity, the ergodic mutual information for M-QAM constellations with equal-probability symbols, the outage probability with and without interference, the secrecy capacity outage probability, and the BER for BPSK modulation, which have been verified by Monte Carlo simulations. It has been shown that for lower K (i.e., lower average ratio of specular to diffuse components power), $\Delta \to 1$ (higher probability of mutual cancellation of the specular component) and lower m_1, m_2 (higher fluctuations of the specular components), the performance worsen for the considered metrics.

The IFTR model can be extended to incorporate the reception of multiple clusters of scattered waves. Such extended model could be used to capture the total received power typically encountered in multi-channel receivers, although at the expense of an increased number of parameters. Such extension is left for future work.

Appendix A
Proof of Lemma I

Let us consider the fading model defined in (3) conditioned to the particular realizations of the RVs $\zeta_1 = u_1$, $\zeta_2 = u_2$. Thus, we can write

$$V_r|_{u_1,u_2} = \sqrt{u}_1 V_1 e^{j\phi_1} + \sqrt{u}_2 V_2 e^{j\phi_2} + X + jY, \tag{52}$$

which corresponds to the TWDP fading model with specular components amplitudes $\sqrt{u}_1 V_1$ and $\sqrt{u}_2 V_2$ and parameters

$$K_{u_1,u_2} = \frac{u_1 V_1^2 + u_2 V_2^2}{2\sigma^2} = u_1 K_1 + u_2 K_2, \tag{53}$$

$$\Delta_{u_1,u_2} = \frac{2\sqrt{u_1 u_2} V_1 V_2}{u_1 V_1^2 + u_2 V_2^2}, \tag{54}$$

which satisfy

$$K_{u_1,u_2}\Delta_{u_1,u_2} = \sqrt{u_1 u_2}\frac{V_1 V_2}{\sigma^2} = \sqrt{u_1 u_2} K\Delta. \tag{55}$$

The conditional average SNR for the model definition given in (52) will be

$$\bar{\gamma}_{u_1,u_2} = \frac{E_s}{N_0}\left(u_1 V_1^2 + u_2 V_2^2 + 2\sigma^2\right) = \frac{E_s}{N_0} 2\sigma^2 \left(1 + K_{u_1,u_2}\right). \tag{56}$$

On the other hand, by promediating over all possible realizations of the unit-mean RVs ζ_1, ζ_2, the unconditional average SNR will be

$$\bar{\gamma} = E\{\bar{\gamma}_{u_1,u_2}\} = \frac{E_s}{N_0}(V_1^2 + V_2^2 + 2\sigma^2) = \frac{E_s}{N_0} 2\sigma^2 (1 + K), \tag{57}$$

and therefore, equating (56) and (57), we can write

$$\frac{1 + K_{u_1,u_2}}{\bar{\gamma}_{u_1,u_2}} = \frac{1}{(E_s/N_0)\, 2\sigma^2} = \frac{1+K}{\bar{\gamma}}, \tag{58}$$

From the PDF of the received power of the TWDP fading model given in [18] as a mixture of Gamma distributions, the PDF of the conditional SNR of the model defined in (52) can be written as

$$\begin{aligned} &f^{\text{TWDP}}_{\gamma_{u_1,u_2}}(x) \\ &= e^{-K_{u_1,u_2}} \sum_{j=0}^{\infty} \frac{K_{u_1,u_2}^j}{j!} f^{\mathcal{G}}\left(x; j+1, \frac{\bar{\gamma}_{u_1,u_2}}{1+K_{u_1,u_2}}\right) \\ &\quad \times \sum_{k=0}^{j} \binom{j}{k} \left(\frac{\Delta_{u_1,u_2}}{2}\right)^k \sum_{l=0}^{k} \binom{k}{l} I_{2l-k}\left(-K_{u_1,u_2}\Delta_{u_1,u_2}\right), \end{aligned} \tag{59}$$

which, from (53)-(58), can be rewritten as

$$\begin{aligned} &f^{\text{TWDP}}_{\gamma_{u_1,u_2}}(x) \\ &= e^{-u_1 K_1 - u_1 K_2} \sum_{j=0}^{\infty} \frac{1}{j!} f^{\mathcal{G}}\left(x; j+1, \frac{\bar{\gamma}}{1+K}\right) \\ &\quad \times \sum_{k=0}^{j} \binom{j}{k} \sum_{q=0}^{j-k} \binom{j-k}{q} (u_1 K_1)^q (u_2 K_2)^{j-k-q} \\ &\quad \times \left(\frac{\sqrt{u_1 u_2} K\Delta}{2}\right)^k \sum_{l=0}^{k} \binom{k}{l} I_{2l-k}\left(-\sqrt{u_1 u_2} K\Delta\right), \end{aligned} \tag{60}$$

The PDF of the SNR of the IFTR model can be obtained by averaging (60) over all possible realizations of the RVs ζ_1 and ζ_2, i.e.

$$f^{\text{IFTR}}_{\gamma}(x) = \int_0^{\infty}\int_0^{\infty} f^{\text{TWDP}}_{\gamma_{u_1,u_2}}(x) f_{\zeta_1}(u_1) f_{\zeta_2}(u_2)\, du_1 du_2, \tag{61}$$

where

$$f_{\zeta_i}(u_i) = \frac{m_i^{m_i} u_i^{m_i-1}}{\Gamma(m_i)} e^{-m_i u_i}, \qquad i = 1, 2. \tag{62}$$

The double integral in (61) can be solved in closed-form by iteratively integrating with respect to variables u_1 and u_2. Thus, after changing the order of integration and summation, we can write

$$f_\gamma^{\text{IFTR}}(x) = \sum_{j=0}^{\infty} f^{\mathcal{G}}\left(x; j+1, \frac{\overline{\gamma}}{1+K}\right) \times \sum_{k=0}^{j} \binom{j}{k} \sum_{q=0}^{j-k} \binom{j-k}{q} \frac{K_1^q K_2^{j-k-q}}{j!} \times \left(\frac{K\Delta}{2}\right)^k \sum_{l=0}^{k} \binom{k}{l} \frac{m_1^{m_1}}{\Gamma(m_1)} \frac{m_2^{m_2}}{\Gamma(m_2)} \mathcal{H}_1, \tag{63}$$

where we have defined

$$\mathcal{H}_1 \triangleq \int_0^\infty u_2^{m_2+j-k/2-q-1} e^{-(m_2+K_2)u_2} \mathcal{I}_1(u_2) du_2, \tag{64}$$

$$\mathcal{I}_1(u_2) \triangleq \int_0^\infty u_1^{m_1+q+k/2-1} e^{-(m_1+K_1)u_1} \times I_{2l-k}\left(-\sqrt{u_1 u_2} K\Delta\right) du_1. \tag{65}$$

We now consider the following equality from [14, 6.643.2] and [14, 9.220.2]:

$$\mathcal{J} = \int_0^\infty t^{\mu-1/2} e^{-pt} I_{2\nu}\left(2\beta\sqrt{t}\right) dt = \frac{\Gamma(\mu+\nu+\frac{1}{2})\beta^{2\nu}}{p^{\nu+\mu+\frac{1}{2}}} \, {}_1\tilde{F}_1\left(\mu+\nu+\frac{1}{2}, 2\nu+1, \frac{\beta^2}{p}\right), \tag{66}$$

where ${}_1\tilde{F}_1$ is the regularized Kummer hypergeometric function, and from which (65) can be written in closed-form as

$$\mathcal{I}_1(u_2) = (-1)^k \frac{\Gamma(m_1+q+l)}{(m_1+K_1)^{m_1+q+l}} \left(\frac{K\Delta}{2}\right)^{2l-k} u_2^{l-k/2} \times {}_1\tilde{F}_1\left(m_1+q+l; 2l-k+1; \frac{u_2 K^2\Delta^2}{4(m_1+K_1)}\right). \tag{67}$$

Introducing (67) into (64) and solving the integral with the help of [14, eq. (7.621.4)] we can write

$$\mathcal{H}_1 = (-1)^k \left(\frac{K\Delta}{2}\right)^{2l-k} \frac{\Gamma(m_1+q+l)}{(m_1+K_1)^{m_1+q+l}} \times \frac{\Gamma(m_2+j-k-q+l)}{(m_2+K_2)^{m_2+j-k-q+l}} \, {}_2\tilde{F}_1\left(m_1+q+l, m_2+j-k-q+l; 2l-k+1; \frac{K^2\Delta^2}{4(m_1+K_1)(m_2+K_2)}\right), \tag{68}$$

which, together with (63), yields the desired result in (8) for the PDF of the SNR of the IFTR fading model. On the other hand, the CDF in (9) is obtained by a simple integration of (8) (see additional comments on this in Section III-B).

APPENDIX B
PROOF OF LEMMA 2: CASE (II)

As in Appendix A, we consider an IFTR model conditioned to the particular realizations of the RVs $\zeta_1 = u_1$, $\zeta_2 = u_2$, which yields a TWDP model with specular components amplitudes $\sqrt{u_1}V_1$ and $\sqrt{u_2}V_2$, parameters K_{u_1,u_2} and Δ_{u_1,u_2} given, respectively, by (53) and (54), and conditional mean $\bar{\gamma}_{u_1,u_2}$, given in (56). The GMGF for the TWDP model for $n \in \mathbb{N}$ can be obtained from [35, eq. (24) for $\mu = 1$] as

$$\phi^{(n)}_{\bar{\gamma}_{u_1,u_2}}(s) = \bar{\gamma}^n_{u_1,u_2} n! e^{\frac{K_{u_1,u_2}\bar{\gamma}_{u_1,u_2}s}{1+K_{u_1,u_2}-\bar{\gamma}_{u_1,u_2}s}} \sum_{q=0}^{n} \binom{n}{q} \frac{K^q_{u_1,u_2}}{q!} \times \frac{(1+K_{u_1,u_2})^{q+1}}{(1+K_{u_1,u_2}-\bar{\gamma}_{u_1,u_2}s)^{q+n+1}} \sum_{r=0}^{q} \binom{q}{r} \left(\frac{\Delta_{u_1,u_2}}{2}\right)^r \times \sum_{l=0}^{r} \binom{r}{l} I_{2l-r}\left(\frac{K_{u_1,u_2}\Delta_{u_1,u_2}\bar{\gamma}_{u_1,u_2}s}{1+K_{u_1,u_2}-\bar{\gamma}_{u_1,u_2}s}\right), \tag{69}$$

which can be written, by using the relations (53)-(58), as

$$\phi^{(\text{n})}_{\gamma_{u_1.u_2}}(s) = \bar{\gamma}^n n! e^{\frac{\bar{\gamma}s}{1+K-\bar{\gamma}s}(u_1K_1+u_2K_2)} \times \sum_{q=0}^{n} \binom{n}{q} \sum_{p=0}^{q-r} \binom{q-r}{p} \frac{(u_1K_1)^p (u_2K_2)^{q-r-p}}{q!} \times \frac{(1+K)^{q+1}}{(1+K-\bar{\gamma}s)^{q+n+1}} \sum_{r=0}^{q} \binom{q}{r} \left(\frac{\sqrt{u_1u_2}K\Delta}{2}\right)^r \times \sum_{l=0}^{l} \binom{r}{l} I_{2l-r}\left(\sqrt{u_1u_2}\frac{K\Delta\bar{\gamma}s}{1+K-\bar{\gamma}s}\right). \tag{70}$$

The GMGF of IFTR fading is obtained by averaging (70) over all possible realizations of ζ_1, ζ_2 as

$$\phi^{(n)}_\gamma(s) = \int_0^\infty \int_0^\infty \phi^{(n)}_{\gamma_{u_1.u_2}}(s) f_{\zeta_1}(u_1) f_{\zeta_2}(u_2) du_1 du_2. \tag{72}$$

Introducing (70) into (72) we can write

$$\phi^{(\text{n})}_{\gamma_{u_1.u_2}}(s) = \bar{\gamma}^n n! \frac{m_1^{m_1}}{\Gamma(m_1)} \frac{m_2^{m_2}}{\Gamma(m_2)} \sum_{q=0}^{n} \binom{n}{q} \sum_{p=0}^{q-r} \binom{q-r}{p} \times \frac{(K_1)^p (K_2)^{q-r-p}}{q!} \frac{(1+K)^{q+1}}{(1+K-\bar{\gamma}s)^{q+n+1}} \sum_{r=0}^{q} \binom{q}{r} \times \left(\frac{K\Delta}{2}\right)^r \sum_{l=0}^{l} \binom{r}{l} \mathcal{H}_2, \tag{73}$$

where we have defined

$$\mathcal{H}_2 \triangleq \int_0^\infty u_2^{m_2+q-r/2-p-1} e^{-\left(m_2-\frac{K_2\bar{\gamma}s}{1+K-\bar{\gamma}s}\right)u_2} \mathcal{I}_2(u_2) du_2, \tag{74}$$

$$\mathcal{I}_2(u_2) \triangleq \int_0^\infty e^{-\left(m_1-\frac{K_1\bar{\gamma}s}{1+K-\bar{\gamma}s}\right)u_1} u_1^{m_1+p+r/2-1}$$

$$\mathcal{H}_2 = (1+K-\overline{\gamma}s)^{m_1+m_2+q}(\overline{\gamma}s)^{2l-r}\left(\frac{K\Delta}{2}\right)^{2l-r}\frac{\Gamma(m_1+l+p)}{(m_1(1+K-\overline{\gamma}s)-K_1\overline{\gamma}s)^{m_1+l+p}} \times \frac{\Gamma(m_2+l-p+q-r)}{(m_2(1+K-\overline{\gamma}s)-K_2\overline{\gamma}s)^{m_2+l-p+q-r}}{}_2\tilde{F}_1\left(m_1+l+p, m_2+l-p+q-r; 2l-r; \frac{(K\Delta\overline{\gamma}s)^2}{4(m_2(1+K-\overline{\gamma}s)-K_2\overline{\gamma}s)(m_1(1+K-\overline{\gamma}s)-K_1\overline{\gamma}s)}\right). \quad (71)$$

$$I_{2l-r}\left(\sqrt{u_1u_2}\frac{K\Delta\bar{\gamma}s}{1+K-\bar{\gamma}s}\right)du_1. \quad (75)$$

Note that $\mathcal{H}_2$ and $\mathcal{I}_2$ are actually the same integrals $\mathcal{H}_1$ and $\mathcal{I}_1$ defined, respectively, in (64) and (65), although for different coefficients, which are now in some cases rational functions on s. Therefore, following the same procedure as in (64)-(68), a closed-form expression can be found for $\mathcal{H}_2$ as given in (71), shown at the top of the page, which together with (73) yields (24).

ACKNOWLEDGMENT

The authors would like to express their gratitude to F. Javier López-Martínez for his insightful comments during the development of this work.

REFERENCES

[1] *Future technology Trends of Terrestrial International Mobile Telecommunications Systems Towards 2030 and Beyond*. Standard Report ITU-R M.2516-0, 2022.

[2] S. Zhang, "An overview of network slicing for 5G," *IEEE Wireless Commun.*, vol. 26, no. 3, pp. 111–117, Jun. 2019.

[3] T. R. R. Marins et al., "Fading evaluation in standardized 5G millimeter-wave band," *IEEE Access*, vol. 9, pp. 67268–67280, 2021.

[4] A. N. Uwaechia and N. M. Mahyuddin, "A comprehensive survey on millimeter wave communications for fifth-generation wireless networks: Feasibility and challenges," *IEEE Access*, vol. 8, pp. 62367–62414, 2020.

[5] T. S. Rappaport et al., "Millimeter wave mobile communications for 5G cellular: It will work!" *IEEE Access*, vol. 1, pp. 335–349, 2013.

[6] M. Pagin, S. Lagén, B. Bojovic, M. Polese, and M. Zorzi, "Improving the efficiency of MIMO simulations in Ns-3," in *Proc. Workshop ns-3*, Jun. 2023, pp. 1–9.

[7] M. Olyaee et al., "The fluctuating two-ray fading model with independent specular components," *IEEE Trans. Veh. Technol.*, vol. 72, no. 5, pp. 5533–5545, 2023.

[8] J. M. Romero-Jerez, F. J. Lopez-Martinez, J. F. Paris, and A. J. Goldsmith, "The fluctuating two-ray fading model: Statistical characterization and performance analysis," *IEEE Trans. Wireless Commun.*, vol. 16, no. 7, pp. 4420–4432, Jul. 2017.

[9] J. Zhang, W. Zeng, X. Li, Q. Sun, and K. P. Peppas, "New results on the fluctuating two-ray model with arbitrary fading parameters and its applications," *IEEE Trans. Veh. Technol.*, vol. 67, no. 3, pp. 2766–2770, Mar. 2018.

[10] M. López-Benítez and J. Zhang, "Comments and corrections to 'new results on the fluctuating two-ray model with arbitrary fading parameters and its applications,"' *IEEE Trans. Veh. Technol.*, vol. 70, no. 2, pp. 1938–1940, Feb. 2021.

[11] M. Olyaee, J. M. Romero-Jerez, F. J. Lopez-Martinez, and A. J. Goldsmith, "Alternative formulations for the fluctuating two-ray fading model," *IEEE Trans. Wireless Commun.*, vol. 21, no. 11, pp. 9404–9416, Nov. 2022.

[12] J. Paris, "Statistical characterization of κ-μ shadowed fading," *IEEE Trans. Veh. Technol.*, vol. 63, no. 2, pp. 518–526, Feb. 2014.

[13] S. Atapattu, C. Tellambura, and H. Jiang, "A mixture gamma distribution to model the SNR of wireless channels," *IEEE Trans. Wireless Commun.*, vol. 10, no. 12, pp. 4193–4203, Dec. 2011.

[14] I. S. Gradshteyn and I. M. Ryzhik, *Table of Integrals, Series, and Products*. New York, NY, USA: Academic, 2014.

[15] G. D. Durgin, T. S. Rappaport, and D. A. de Wolf, "New analytical models and probability density functions for fading in wireless communications," *IEEE Trans. Commun.*, vol. 50, no. 6, pp. 1005–1015, Jun. 2002.

[16] A. Abdi, W. C. Lau, M.-S. Alouini, and M. Kaveh, "A new simple model for land mobile satellite channels: First-and second-order statistics," *IEEE Trans. Wireless Commun.*, vol. 2, no. 3, pp. 519–528, May 2003.

[17] L. Moreno-Pozas, F. J. Lopez-Martinez, J. F. Paris, and E. Martos-Naya, "The κ–μ shadowed fading model: Unifying the κ–μ and η–μ distributions," *IEEE Trans. Veh. Technol.*, vol. 65, no. 12, pp. 9630–9641, Dec. 2016.

[18] N. Y. Ermolova, "Capacity analysis of two-wave with diffuse power fading channels using a mixture of gamma distributions," *IEEE Commun. Lett.*, vol. 20, no. 11, pp. 2245–2248, Nov. 2016.

[19] M. Vetterli, J. Kovačević, and V. K. Goyal, *Foundations of Signal Processing*. Cambridge, U.K.: Cambridge Univ. Press, 2014.

[20] A. Papoulis, *Random Variables and Stochastic Processes*. New York, NY, USA: McGraw-Hill, 1994.

[21] M. K. Samimi, G. R. MacCartney, S. Sun, and T. S. Rappaport, "28 GHz millimeter-wave ultrawideband small-scale fading models in wireless channels," in *Proc. IEEE 83rd Veh. Technol. Conf. (VTC Spring)*, May 2016, pp. 1–6.

[22] P. Ramírez-Espinosa and F. J. López-Martínez, "Composite fading models based on inverse gamma shadowing: Theory and validation," *IEEE Trans. Wireless Commun.*, vol. 20, no. 8, pp. 5034–5045, Aug. 2021.

[23] M. Rao, F. J. Lopez-Martinez, M.-S. Alouini, and A. Goldsmith, "MGF approach to the analysis of generalized two-ray fading models," *IEEE Trans. Wireless Commun.*, vol. 14, no. 5, pp. 2548–2561, May 2015.

[24] M.-S. Alouini and A. Goldsmith, "Capacity of Nakagami multipath fading channels," in *Proc. IEEE 47th Veh. Technol. Conference. Technol. Motion*, 1997, pp. 358–362.

[25] F. Yilmaz and M.-S. Alouini, "Novel asymptotic results on the high-order statistics of the channel capacity over generalized fading channels," in *Proc. IEEE 13th Int. Workshop Signal Process. Adv. Wireless Commun. (SPAWC)*, 2012, pp. 389–393.

[26] M. Abramowitz and I. A. Stegun, *Handbook of Mathematical Functions With Formulas, Graphs, and Mathematical Tables*, 10th ed. Gaithersburg, MD, USA: U.S. Department of Commerce-NBS, Dec. 1972.

[27] C. Ouyang, S. Wu, C. Jiang, D. W. K. Ng, and H. Yang, "Receive antenna selection under discrete inputs: Approximation and applications," *IEEE Trans. Commun.*, vol. 68, no. 4, pp. 2634–2647, Apr. 2020.

[28] J. Romero-Jerez and A. Goldsmith, "Receive antenna array strategies in fading and interference: An outage probability comparison," *IEEE Trans. Wireless Commun.*, vol. 7, no. 3, pp. 920–932, Mar. 2008.

[29] F. Javier López-Martínez, E. Martos-Naya, J. F. Paris, and U. Fernández-Plazaola, "Generalized BER analysis of QAM and its application to MRC under imperfect CSI and interference in Ricean fading channels," *IEEE Trans. Veh. Technol.*, vol. 59, no. 5, pp. 2598–2604, Jun. 2010.

[30] M. K. Simon and M.-S. Alouini, *Digital Communications Over Fading Channels*, 2nd ed. Hoboken, NJ, USA: Wiley, 2005.

[31] Z. Wang and G. B. Giannakis, "A simple and general parameterization quantifying performance in fading channels," *IEEE Trans. Commun.*, vol. 51, no. 8, pp. 1389–1398, Aug. 2003.

[32] M. Bloch, J. Barros, M. R. Rodrigues, and S. W. McLaughlin, "Wireless information-theoretic security," *IEEE Trans. Inf. Theory*, vol. 54, no. 6, pp. 2515–2534, Jun. 2008.

[33] J. M. Romero-Jerez, G. Gomez, and F. J. Lopez-Martinez, "On the outage probability of secrecy capacity in arbitrarily-distributed fading channels," in *Proc. 21st Eur. Wireless Conf.*, 2015, pp. 1–6.

[34] J. P. Pena-Martin, J. M. Romero-Jerez, and F. J. Lopez-Martinez, "Generalized MGF of Beckmann fading with applications to wireless communications performance analysis," *IEEE Trans. Commun.*, vol. 65, no. 9, pp. 3933–3943, Sep. 2017.

[35] M. Olyaee, J. P. Peña-Martín, F. J. Lopez-Martinez, and J. M. Romero-Jerez, "Statistical characterization of the multicluster two-wave fading model," in *Proc. 5th Int. Conf. Adv. Commun. Technol. Netw. (CommNet)*, Dec. 2022, pp. 1–7.

Maryam Olyaee received the B.Sc. degree in electrical engineering from Shahed University, Tehran, Iran, in 2014, and the M.Sc. and Ph.D. degrees in electrical engineering from Shiraz University of Technology, Shiraz, Iran, in 2016 and 2021, respectively. She was a Post-Doctoral Researcher with the University of Malaga, Spain, from March 2021 to August 2022, and the University of Granada, Spain, from September 2022 to February 2023. She is currently a Senior Researcher with the University of Malaga. Her research interests include wireless and cellular communications, multiuser MIMO/MIMO-OFDM, massive MIMO systems, reconfigurable intelligent surfaces (RIS), green communications, and mm-Wave communications for 5G and beyond.

Hadi Hashemi received the B.Sc. degree in electrical engineering from the University of Urmia in 2012, the M.Sc. degree in electrical engineering from Imam Khomeini International University in 2014, and the Ph.D. degree in communications from Shiraz University of Technology in 2021. He was a Visiting Researcher with the University of Malaga, Spain, from September 2022 to February 2023. He is currently a Post-Doctoral Researcher with the University of Granada, Spain. His research interests include cooperative communications, wireless sensor networks, cognitive radio networks, channel modeling, satellite communication, and next-generation mobile networks.

Juan M. Romero-Jerez (Senior Member, IEEE) received the M.Sc. degree in telecommunications engineering and mathematics and the Ph.D. degree in telecommunications engineering from the University of Malaga, Spain, in 2001. In 1996, he joined the Department of Electronic Technology, University of Malaga, where he is currently a Full Professor. He was a Visiting Associate Professor with the Department of Electrical Engineering, Stanford University, from September 2005 to February 2006, from September 2007 to February 2008, and from February 2016 to March 2016. He has participated in several research projects in the areas of packet radio transmission, multiple antennas, interference management, and cellular networks. His current research interests include wireless communications and more specifically: wireless communications performance analysis, multipath fading, wireless channel modeling, diversity systems, smart antennas, MIMO performance, and interference management. He was the General Co-Chair of the 2022 IEEE Communication Theory Workshop (CTW 2022). He was an Editor of IEEE TRANSACTIONS ON WIRELESS COMMUNICATIONS from 2015 to 2020.